

Review

# The anions and dianions of group 14 metalloles

Masaichi Saito\*, Michikazu Yoshioka

*Department of Chemistry, Faculty of Science, Saitama University, Shimo-okubo, Sakura-ku, Saitama-city, Saitama, 338-8570, Japan*

Received 15 April 2004; accepted 22 June 2004

Available online 19 November 2004

## Contents

1. Introduction .....	765
2. Earlier studies .....	766
3. Theoretical studies on metallole anions .....	766
4. Synthesis and structures of silole anions .....	767
4.1. Silole anions .....	767
4.2. Benzannulated silole anions .....	768
5. Synthesis and structures of germole anions .....	769
6. Theoretical studies on metallole dianions .....	769
7. Synthesis and structures of silole and germole dianions .....	770
7.1. Silole dianions .....	770
7.2. Germole dianions .....	771
8. Synthesis and structures of benzannulated silole and germole dianions .....	772
8.1. Metallaindene dianions .....	772
8.2. Metallafluorene dianions .....	773
9. $\eta^5$ -Sila- and germacyclopentadienyl transition metal complexes .....	775
9.1. Synthesis, structures, and properties .....	775
9.2. Reactivity .....	776
10. Synthesis and reactions of stannole anions and dianions .....	777
11. Conclusion .....	778
Acknowledgments .....	778
References .....	779

## Abstract

The synthesis, structures, and physical and chemical properties of mono- and dianions of group 14 metalloles (1-metallacyclopentadiene), heavier congeners of the cyclopentadienyl anion, are described. Dianions of metalloles have a substantial aromatic character owing to strong participation of divalent resonance forms and the silole anion shows different degrees of aromaticity depending on the substituent, but there is no evidence for aromaticity in the germole anion. Dianions of benzannulated metalloles have more aromatic character in the metallole ring than in the benzene ring. The synthesis and characterization of  $\eta^5$ -silolyl and  $\eta^5$ -germolyl metal complexes, analogs of ferrocene, and their unique reactivity are also described.

© 2004 Elsevier B.V. All rights reserved.

**Keywords:** Cyclopentadienyl anion; Aromaticity; Metal complexes

## 1. Introduction

The five-membered heterocyclic dienes **1** such as pyrrole, furan, and thiophene have played an important role in

\* Corresponding author. Tel.: +81 48 858 9029; fax: +81 48 858 3700.  
E-mail address: [masaichi@chem.saitama-u.ac.jp](mailto:masaichi@chem.saitama-u.ac.jp) (M. Saito).

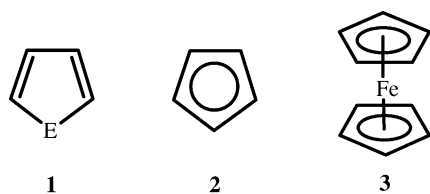


Plate 1.

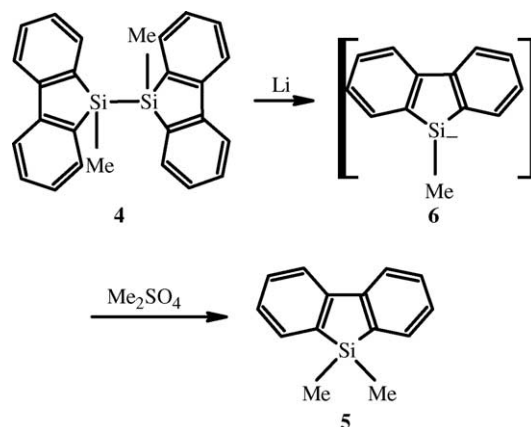
heterocyclic chemistry. The rings are generally named heterocyclopentadiene, heteroles, or metalloles according to the non-metallic or metallic character of E. Derivatives of pyrrole, furan, and thiophene, so-called heteroaromatic compounds, are well investigated as building blocks of electrical conductors as well as natural products. Cyclopentadienyl anion **2**, a conjugated base of cyclopentadiene, is a well-known aromatic species and is widely used as a ligand in transition metal complexes such as ferrocene **3** (Plate 1).

Since the first isolation of stable compounds with Sn=Sn [1], Si=Si [2], and P=P [3] bonds, a large number of stable compounds having a double bond containing heavier group 14 elements have been reported and many comprehensive reviews have been published (For examples of reviews, see [4]). The study of delocalized  $\pi$ -systems containing these bonds is of interest because of expected new chemical and electronic properties. Very recently, the synthesis of anions and dianions of group 14 metalloles, heavier congeners of the cyclopentadienyl anion, has received much attention. A few reviews on anionic and coordination species of group 14 metalloles have already appeared [5]. The present review is focused upon a historical survey of the chemistry of anions and dianions of group 14 metalloles from the standpoint of aromaticity together with our recent work on the synthesis and reactions of stannole mono- and dianions.

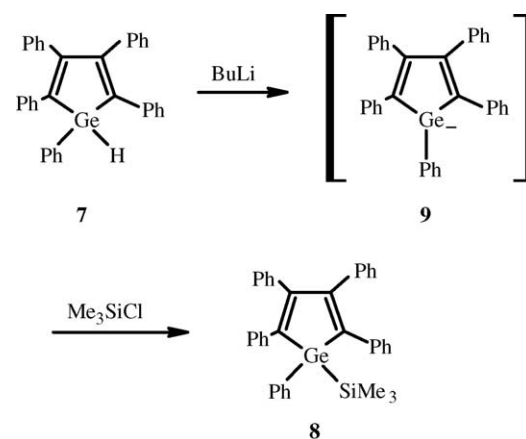
## 2. Earlier studies

The first silacyclopentadienyl anion was prepared by Gilman in 1958 [6]. After treatment of 5,5-dimethylbi(5,5-dibenzosilole) **4** with lithium, the resulting mixture was allowed to react with dimethyl sulfate to afford 5,5-dimethylbenzosilole **5**, suggesting the formation of intermediary dibenzosilole anion **6** (Scheme 1).

The first synthesis of a germole anion was reported by Curtis in 1967 [7]. Reaction of 1-phenylgermole **7** with butyllithium gave a bright red solution. Treatment of the resulting solution with chlorotrimethylsilane afforded 1-phenyl-1-trimethylsilylgermole **8**. Thus, the bright red color was ascribed to germole anion **9** (Scheme 2). In earlier studies, the generation of such anionic species was evidenced by trapping experiments. The electronic properties of these anions were not clarified by these studies.



Scheme 1.



Scheme 2.

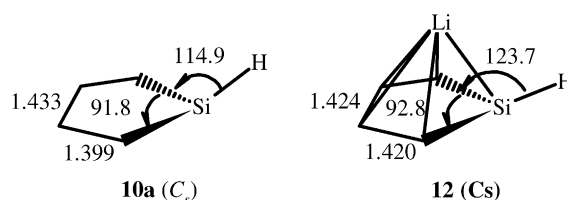


Fig. 1. Comparison of calculated structures of **10a** and **12** (RMP2(fc)/6-31G\*\* level, bond lengths in angstroms, angles in degrees).

## 3. Theoretical studies on metallole anions

Theoretical calculations using RMP2(fc)/6-31G\*\* level [8] showed that the silole anion **10a** has a strongly flattened pyramidal silicon center (angle sum  $321.6^\circ$ ) relative to  $\text{SiH}_3^-$  (RMP2/6-31G\*\*, angle sum  $289.3^\circ$ ) (Fig. 1). The inversion barrier (from **10a** to **10b**) is low, 3.8 kcal/mol (Plate 2). The

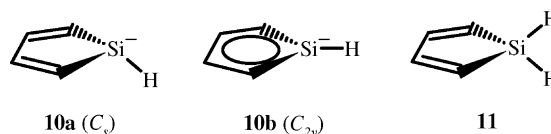


Plate 2.

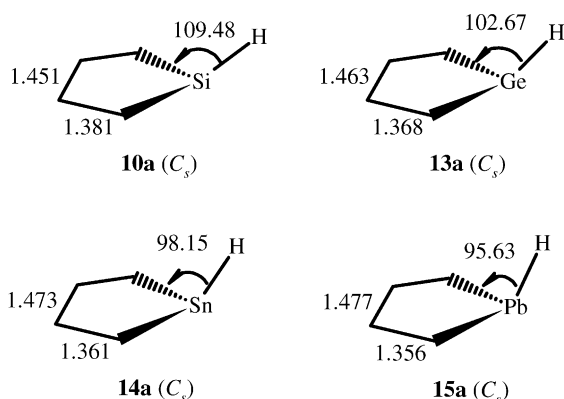


Fig. 2. Optimized geometries (B3LYP/6-31+G\* (C, H), /LanL2DZdp (E)) of metallole anions ( $C_s$ ). Bond lengths are given in angstroms and angles in degrees.

bond length difference between  $C_\alpha-C_\beta$  and  $C_\beta-C_\beta$  in **10a** (0.034 Å) is significantly reduced relative to that in the neutral **11** (0.124 Å) suggesting that the negative charge in the ground state of **10a** should be delocalized. The anion **10a** exhibits a large Julg parameter ( $A = 0.971$ ), while that of **11** is 0.608 [9,10]. The coordination of lithium to the silole ring influences the structure. The silicon environment in lithium silolide **12** is significantly less pyramidal than that in **10a** and the sum of the angles at silicon increases by 18.6° (Fig. 1). The C–C bond lengths have nearly the same length ( $A = 0.9996$ ). Consequently, lithium coordination enhances delocalization in the silole ring. The aromatic stabilization energy (denoted as ASE hereafter) in **12** corresponds to 80% of that computed for  $Li^+C_5H_5^-$ , whereas ASE in **10a** is 55% of that for  $C_5H_5^-$ .

Comprehensive work on the calculation for metallole anions was later reported [11]. Pyramidity at the trivalent Group 14 elements in the metallole anion with  $C_s$  symmetry increases as the element goes from C to Pb with decreased conjugation and increased C–C bond length alternations (Fig. 2).

The inversion barriers of  $C_s$  to  $C_{2v}$  increase from C to Pb, although they are lower than those of the corresponding dimethyl anions. Relative to the dimethyl anions, the inversion barriers of  $C_s$  to  $C_{2v}$  are more substantially reduced for Si (26.6 kcal/mol) and Ge (25.9 kcal/mol) than those for Sn (18.4 kcal/mol) and Pb (20.1 kcal/mol). The isodesmic stabilization energies of the planar  $C_{2v}$  anions are lower than those of the pyramidal  $C_s$  anions, and hence the planar structures have higher aromatic character than the pyramidal structures (Fig. 3).

## 4. Synthesis and structures of silole anions

### 4.1. Silole anions

The first NMR characterization of a silole anion was reported by Boudjouk and Hong in 1993 [12]. The synthesis of

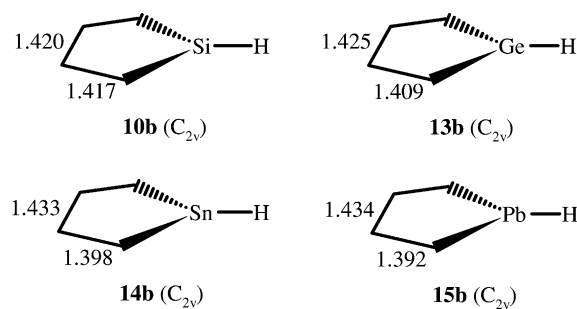
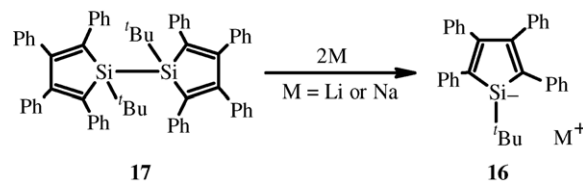


Fig. 3. Optimized geometries (B3LYP/6-31+G\* (C, H), /LanL2DZdp (E)) of planar metallole anions ( $C_{2v}$ ). Bond lengths are given in angstroms.



Scheme 3.

silole anion **16** was accomplished by the reduction of bi(1,1-silole) **17** with alkali metal (Scheme 3).

The  $^{29}Si$  NMR chemical shift of **16** was observed at 26.12 ppm, a large downfield shift compared to that of **17** (3.62 ppm), although upfield shifts were reported when organosilanes were converted to silyl anions [13]. Such downfield shifts were also observed in phospholyl anions. Their  $^{31}P$  resonances are located at 60–80 ppm, downfield compared to those of neutral phospholes, reflecting the delocalization of the negative charge [14]. The downfield resonance of **16** in  $^{29}Si$  NMR would be ascribed to the diffusion of silicon p-orbitals and/or delocalization of the negative charge into the butadiene moiety, so as to show aromaticity (Plate 3). The contribution of resonance forms would result in the increase of  $\pi$ -electron density on  $\alpha$ - and  $\beta$ -carbons to affect the  $^{13}C$  chemical shifts. In fact, the  $^{13}C$  NMR signals assigned to these carbon centers were observed upfield of those from the starting material.

C-Alkylated silole anions were also synthesized and characterized [15,16]. Nucleophilic cleavage of an Si–Si bond of 1,1-bis(trimethylsilyl)silole **17** with benzylpotassium in the presence of 18-crown-6 gave C-methylated silole anion **18**. The  $^{29}Si$  NMR resonance for **18** (−41.52 ppm) is shifted upfield relative to the corresponding resonance of the parent silole **17** (−34.26 ppm) and appears in the region expected

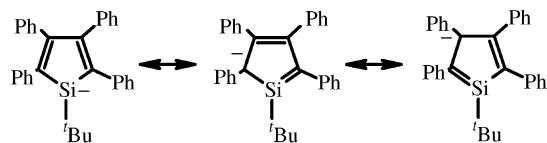
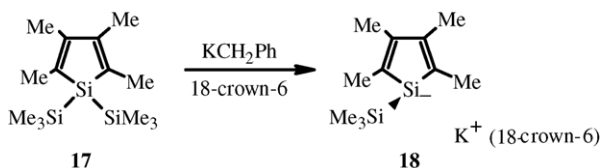
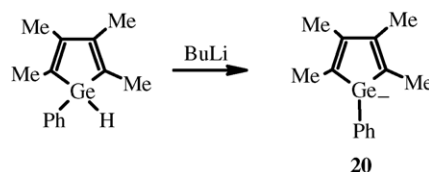


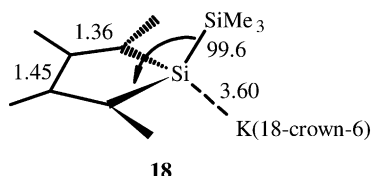
Plate 3.



Scheme 4.



Scheme 5.

Fig. 4. Structure of **18**. Bond lengths are given in angstroms and angles in degrees.

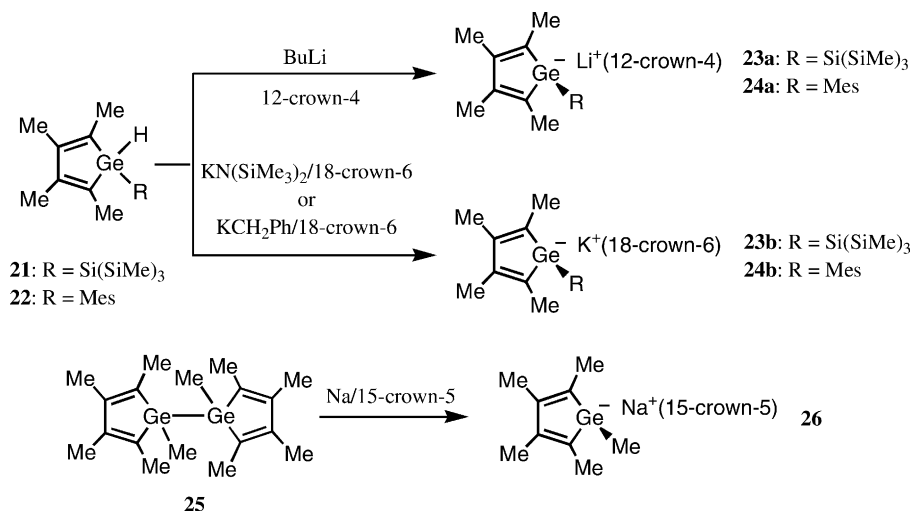
for classical silyl anions [17]. This trend is completely opposite to that reported for the C-phenylated silole anion formed from the bi(1,1-silole). The negative charge of C-alkylated silole is localized on the silicon (Scheme 4). The opposite distribution of the negative charge may be due to modes of substitution (phenyl versus methyl) in the ring and/or to the degrees of interaction between the alkali metal cation and the silole ring.

X-ray structural analysis of silole anion **18** [16] indicates that the anion is non-aromatic as indicated by the pronounced bond alternation. The difference between the  $C_\alpha-C_\beta$  and  $C_\beta-C_\beta$  distances is nearly 0.1 Å. The angle of  $99.6^\circ$  between the  $C_4Si$  plane and the Si-Si bond also indicates a high degree of pyramidalization at the silicon to decrease conjugation. The  $[K(18\text{-crown-6})]^+$  cation interacts weakly with the silicon (3.4 Å). The distance of K from the tetrahedral silicon provides further evidence for the non-aromaticity of **18** (Fig. 4). Thus, the substituents on the silole ring carbon play an important role for the aromaticity of the silole anion.

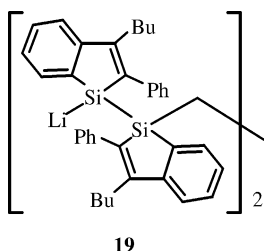
#### 4.2. Benzannulated silole anions

Estimation of the degree of aromaticity of dibenzosilole anions is of interest because the acidity of cyclopentadiene ( $pK_a = 16$ ) is attenuated in the fused ring analog fluorene ( $pK_a = 23$ ) as a result of reduced  $\pi$ -delocalization in the conjugate base of the annulated system [18]. About 40 years after the first report on the synthesis of a dibenzosilole anion by Gilman, a dibenzosilole anion (1-silafluorenyl anion) was characterized by NMR and its aromaticity was discussed [19]. Sonication of bis(1-methyl-1-silafluorenyl) **4** and lithium in THF gave a dark green solution of silafluorenyl anion **6** (Scheme 1). The  $^{29}\text{Si}$  NMR chemical shift for **6** ( $-22.09$  ppm) is in the range of aryl-substituted silyl-lithiums [13a,20]. Upon metallation of **4** to **6**, the  $^{13}\text{C}$  signals for the  $C_\alpha$  and  $C_\beta$  of the ring and methyl carbon shifted to downfield. Since the  $C_{\text{ipso}}$  and the methyl carbon of  $\text{Ph}_2\text{MeSi}^-\text{Li}^+$  also appeared downfield relative to  $\text{Ph}_2\text{MeSiCl}$  [13a], the downfield shifts of **6** are explained in terms of a field effect induced by the negative charge on the silicon [21]. Therefore, the negative charge of **6** is localized on the silicon. The annulation essentially affects  $\pi$ -localization.

X-ray structural analysis of benzosilole anion **19** was also reported [22]. Since the benzene ring of **19** has a slightly distorted diene character with the C-C bond lengths of 1.35–1.49 Å, the silole ring is essentially non-aromatic.



Scheme 6.



## 5. Synthesis and structures of germole anions

After the pioneering work on the synthesis of C-phenylated germole anions by Curtis [7] and Jutzi [23], C-methylated 1-phenylgermole anion **20** stable in solution was synthesized by the reaction of 1-phenylgermole with butyllithium (Scheme 5) [24]. The deshielding of  $C_\alpha$  and  $C_\beta$  was observed and attributed to the highly localized negative charge on germanium. The  $C_{ipso}$  of 1-phenyl group resonated at low field compared to that of the starting germole as observed in phenylgermanes and their anions [25].

X-ray structural analyses of the C-methylated germole anions later appeared [16,26]. Deprotonation of **21** and **22** with butyllithium in the presence of a crown ether produced 1-tris(trimethylsilyl)silylgermole anion **23a** and 1-mesitylgermole anion **24a**, respectively (Scheme 6). The potassium derivatives, **23b** and **24b**, were also synthesized from **21** and **22**, respectively (Scheme 6). Reductive cleavage of the Ge–Ge bond in bi(1,1-germole) **25** with Na/15-crown-5 produced 1-methylgermole anion **26** (Scheme 6).

The  $^{13}\text{C}$  NMR signals for the ring carbon centers of the anions are somewhat downfield relative to those for the starting compounds. These anions may be a non-aromatic species with the negative charge localized on the germanium. All anions characterized by X-ray analysis possess a pyramidal germanium center with a sharp angle between the  $C_4\text{Ge}$  plane and the Ge–M (M = C, Si) bond. Furthermore, the  $C_4$  moiety of the ring has considerable diene character as indicated by the C–C bond lengths. Thus, the experimental data reveal the non-aromatic nature of germole anions with significant localization of the negative charge on germanium.

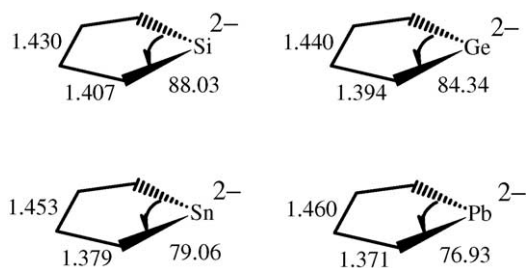


Fig. 5. Optimized geometries (B3LYP/6-31+G\* (C, H), /LanL2DZdp (E)) of  $\text{C}_4\text{H}_4\text{E}^{2-}$  ( $\text{C}_{2v}$ ). Bond lengths and angles are given in angstroms and degrees respectively.

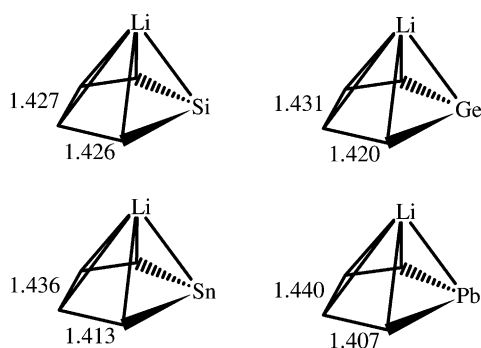


Fig. 6. Optimized geometries (B3LYP/6-31+G\* (C, H), /LanL2DZdp (E)) of lithium metalloyl anions **27** ( $\text{C}_s$ ). Bond lengths are given in angstroms.

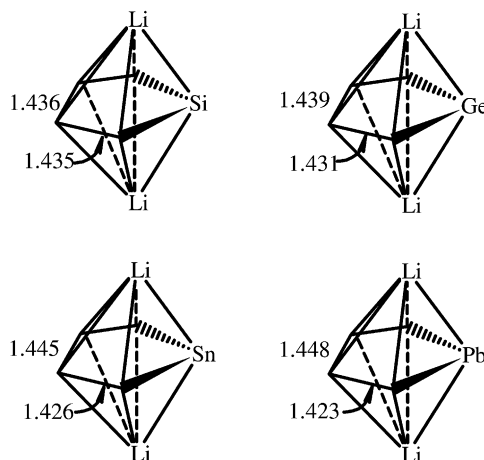


Fig. 7. Optimized geometries (B3LYP/6-31+G\* (C, H), /LanL2DZdp (E)) of dilithium metallole **28** ( $\text{C}_{2v}$ ). Bond lengths are given in angstroms.

## 6. Theoretical studies on metallole dianions

The lower aromaticity of the silole anion **10a** relative to the cyclopentadienyl anion is due to the pyramidal ground-state geometry around the silicon center resulting in poor conjugation. The overlap of 2p and 3p orbitals is not inherently poor [27]. Hence, the reduced pyramidalization or complete planarity should result in increased overlap and better conjugation in the silole anion. Indeed, the decreased pyramidalization at the silicon in lithium silolide **12** results in enhanced aromaticity (Fig. 1) [28].

The pyramidalization problem does not arise in the metallole dianions. The C–C distances in calculated geometries of free metallole dianions are shown in Fig. 5. Relative to the free dianions,  $\eta^5\text{-Li}^+$  complexation results in more equalized C–C distances in both lithium **27** and dilithium derivatives **28** (Figs. 6 and 7). The lithium metalloyl anion **27** and dilithium metallole **28** should have considerable aromaticity.

Nucleus-independent chemical shifts (NICS) computed at the ring centers (non-weighted mean of the heavy atom coordinates) are efficient probes for dia- and paratropic ring currents, associated with aromaticity and anti-aromaticity, respectively [29]. The calculated negative NICS values of



Table 1

Nucleus-independent chemical shifts (NICS's; ppm)<sup>a</sup> and <sup>7</sup>Li NMR chemical shifts (ppm)<sup>b</sup> of dilithium metalloles **28**

	Si	Ge	Sn	Pb
NICS	−0.53	−5.41	−6.88	−10.04
$\delta$ ( <sup>7</sup> Li)	−9.0	−8.1	−6.7	−6.0

<sup>a</sup> GIAO-SCF/6-31+G\* (C, H), /6-31G\* (Li) [/6-311+G\* for  $\delta$  (<sup>7</sup>Li)], /LanL2DZdp (E).

<sup>b</sup> Li<sup>+</sup>(H<sub>2</sub>O)<sub>4</sub>,  $\sigma$  (Li) = 91.9.

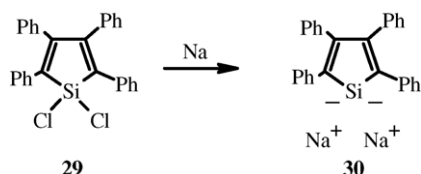
dilithium metalloles **28** reflect a high degree of aromaticity (Table 1). The considerable <sup>7</sup>Li shieldings in **28** (Table 1) are diagnostic of the aromatic ring current [30].

## 7. Synthesis and structures of silole and germole dianions

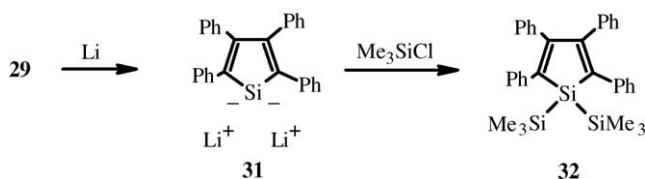
### 7.1. Silole dianions

The first synthesis of a silole dianion was accomplished by the reaction of 1,1-dichlorosilole **29** with sodium (Scheme 7) [31]. Minimal differences in the <sup>13</sup>C NMR chemical shifts of the silole dianion **30** and dichlorosilole **29** indicate that the negative charges of **30** are localized on silicon.

Four years after the pioneering work by Joo, the NMR data of silole dianion **31** were reported and its aromaticity was discussed (Scheme 8) [32]. Sonification of **29** with more than 4 equivalents of lithium followed by quenching with chlorotrimethylsilane gave 1,1-bis(trimethylsilyl)silole **32**, suggesting the formation of silole dianion **31**. An NMR study of the reaction mixture of **29** and excess lithium revealed the presence of only one species assignable to silole dianion **31**. The <sup>29</sup>Si NMR spectrum showed only one resonance at 68.54 ppm, remarkably downfield compared to that of the starting **29** (6.80 ppm). In <sup>13</sup>C NMR spectrum, the signals due to the C<sub>α</sub> and C<sub>β</sub> atoms in the ring were observed upfield. Upfield shifts are generally observed for five-membered ring compounds having aromatic contributors such as cyclopentadienyl anions [33] and Group 15 heterole anions [33,34] relative to the corresponding neutrals. The upfield shifts for



Scheme 7.



Scheme 8.

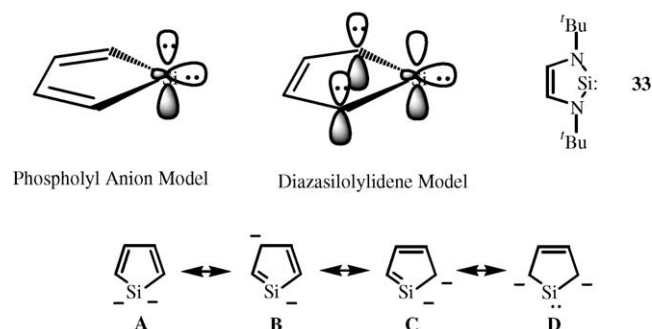
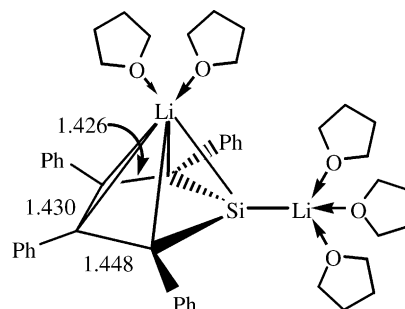


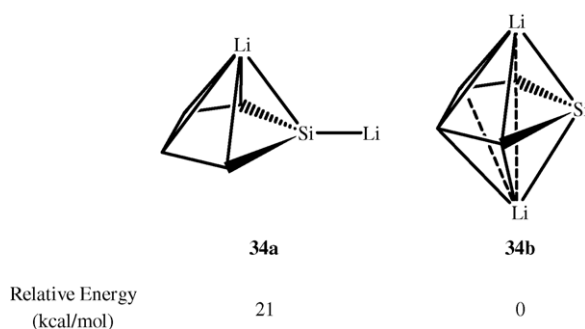
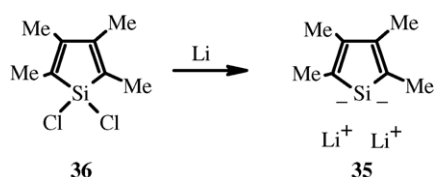
Plate 4.

the C<sub>α</sub> and C<sub>β</sub> in the <sup>13</sup>C NMR spectrum and the downfield shift in the <sup>29</sup>Si NMR are consistent with significant charge delocalization from silicon onto the ring.

Two reasonable models for understanding the electronic structure of **31** were proposed. One is the phosphoryl anion model having a structure isoelectronic with **31** (Plate 4). The phosphoryl anions have <sup>31</sup>P NMR resonances 60–80 ppm downfield from the neutral phospholes [14]. The electronic structure of the phosphoryl anion is similar to that of cyclopentadienyl anion [35]. The other is the cyclic silylene model having a conjugated 6π-electron system, namely, 1,3-di-*t*-butyl-2,3-dihydro-1H-1,3,2-diazasilol-2-ylidene **33** [36], where the silicon atom shares nearly pure p orbitals with the neighboring nitrogen atoms and has an s orbital to hold a lone pair (Plate 4). The molecular orbital model of **31** is better approximated by the diazasilolylidene species because an <sup>29</sup>Si NMR resonance of **33** is observed at 78.3 ppm (68.54 ppm for **31**). Thus, the resonance form **D** was proposed as a major contributor in **31** because the electronic density of **31** was consistent with that interpreted by NMR data (<sup>29</sup>Si = 68.54 ppm, upfield shifts of C<sub>α</sub> and C<sub>β</sub>). According to the theoretical calculation, however, the reported assignments of C<sub>α</sub> and C<sub>β</sub> should be reversed [28].

Silole dianion **31** was isolated in a crystalline form from THF (Fig. 8) [37]. The structure of **31** contains two different lithium atoms. One lithium atom is η<sup>5</sup>-bonded to the silole ring and coordinated to two THF molecules. The other is η<sup>1</sup>-bonded to the silicon atom and coordinated to three THF molecules. The ring C–C distances are nearly equal in the range 1.426–1.448 Å.

Fig. 8. X-ray structure of **31**. Bond lengths are given in angstroms.

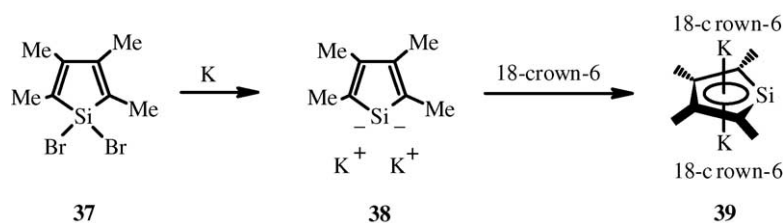
Fig. 9. Calculated structure for  $\text{Li}_2(\text{C}_4\text{H}_4)\text{Si}$  **34**.

Scheme 9.

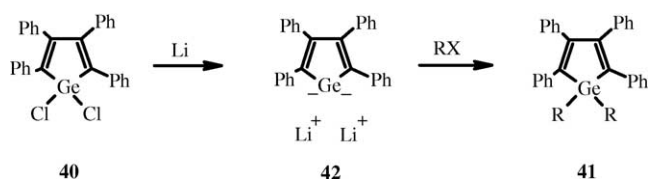
To explore the structure of **31**, theoretical calculations of the dilithium salt of unsubstituted silole **34** were carried out. Two different dilithio complexes were found to be optimum structures, **34a** and **34b**. The structure **34a** corresponds closely to the X-ray structure. The other structure **34b** has two  $\eta^5$ -coordinated lithium centers on both sides of the ring and is more stable than **34a** by 21 kcal/mol (Fig. 9). As already mentioned, the structure of **31** has two different lithium atoms as shown in **34a** in the solid state. However, **34a** might change to thermodynamically more stable **34b** in solution. The  $^7\text{Li}$  NMR of **31** showed a single resonance at 0.23 ppm. This suggests the presence of only **34b** or rapid inter- or intramolecular exchange of the lithium cations between nonequivalent sites in **34a**.

The C-methylated silole dianion **35** was also synthesized by the reduction of the corresponding 1,1-dichlorosilole **36** and characterized by NMR studies (Scheme 9) [38]. The  $^{29}\text{Si}$  resonance in **35** was shifted downfield compared to that of **36** due to delocalization of its negative charge into the silole ring. The  $^{13}\text{C}$  NMR spectrum of **35** showed peaks due to the ring carbons in upper field than those of **36** and was interpreted in terms of some aromatic character of **35**, although the assignment is still controversial [28].

Reduction of 1,1-dibromosilole **37** in THF with potassium produced dianion **38**, which was isolated in crystalline form



Scheme 10.



Scheme 11.

as a complex **39** with 18-crown-6 (Scheme 10) [15,16]. X-ray analysis of **39** revealed the very slight bond length alternation in the silole ring also due to considerable delocalization of  $\pi$ -electron density. In contrast to the structure of **31**, the metals in **39** occupy an  $\eta^5$ -position on both sides of the ring.

## 7.2. Germole dianions

The first synthesis of a germole dianion was accomplished by the reaction of 1,1-dichlorogermylene **40** with lithium [39]. Sonication of **40** with lithium in THF gave a dark-red solution. Addition of the resulting solution to RX produced **41**, suggesting the formation of germole dianion **42** (Scheme 11). Monitoring the reduction of **40** with lithium by NMR revealed the presence of only one species assignable to **42**, whose  $\text{C}_\alpha$  shifted upfield and  $\text{C}_\beta$  shifted downfield. These shifts were rationalized in terms of the strong contribution of a resonance form where the  $\alpha$ -carbons were negatively charged and the germanium was divalent, like the resonance form **D** in silole dianion **31** (Plate 4). The assignments, however, were afterwards revised such that the downfield- and upfield-shifted signals were due to  $\text{C}_\alpha$  and  $\text{C}_\beta$ , respectively [40].

The dilithio complex **42** crystallized from dioxane in two structurally distinct forms, depending on the crystallization temperature (Fig. 10) [41]. The crystal structure of **42a** (crystals obtained from dioxane at  $-20^\circ\text{C}$ ) has a reverse-sandwich structure. The two lithium atoms are coordinated to two dioxane molecules and lie on both sides of the germole ring. The crystals of **42b**, obtained at  $25^\circ\text{C}$  have two structurally different lithium atoms; one is  $\eta^5$ -coordinated to the ring and the other is  $\eta^1$ -coordinated to the germanium atom. In both structures, the ring electrons are highly delocalized leading to nearly equal C–C bond lengths. There is a significant difference between the structures of **31** and **42b**. In **31** the arrangement at the silicon center is nearly planar, whereas in **42b** the  $\eta^1$ -coordinated lithium center is shifted to the hemisphere anti to the  $\eta^5$ -coordinated lithium center. The

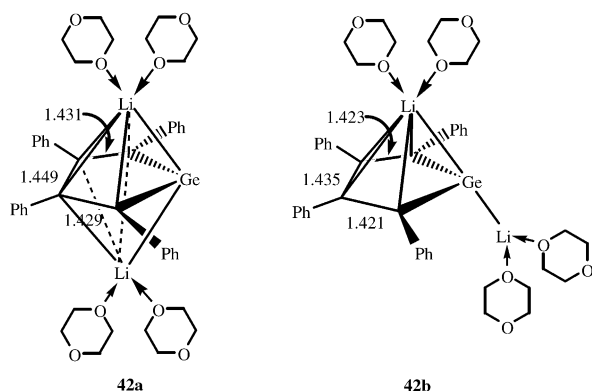
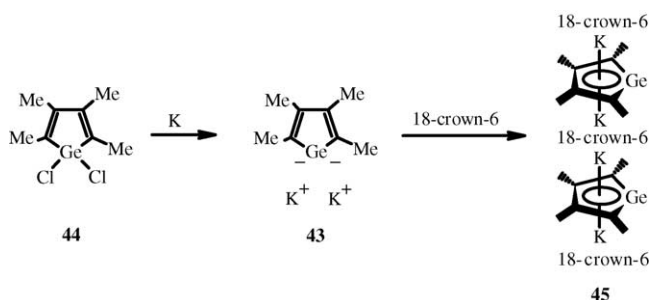


Fig. 10. X-ray structure of **42**. Bond lengths are given in angstroms.



Scheme 12.

angle between the Li–Ge vector and the C–Ge–C plane is  $42.9^\circ$ . The MO calculations of  $\text{Li}_2(\text{H}_4\text{C}_4\text{Ge})$  revealed that the type **42a** structure was more stable than the type **42b** structure by 25 kcal/mol. The aromatic stabilization energy of  $(\text{H}_4\text{C}_4\text{Ge})^{2-}$  was predicted to be 13 kcal/mol and hence the germole dianion should be aromatic.

The C-methylated germole dianion **43** was synthesized by the reduction of 1,1-dichlorogermole **44** with potassium (Scheme 12) [16]. The dianion **43** crystallized in the presence of 18-crown-6 as the bis(germole dianion) complex **45**, which was characterized by X-ray analysis. The slight differences in the C–C bond lengths in the  $\text{C}_4\text{Ge}$  ring suggest considerable delocalization of  $\pi$ -electron density in the ring.

The C-ethylated germole dianion was also synthesized by the reaction of the corresponding 1,1-dichlorogermole with lithium and its unique structure was established by X-ray analysis (Fig. 11) [42]. Reaction of 1,1-dichlorogermole with lithium in THF gave a dark red solution of germole dianion

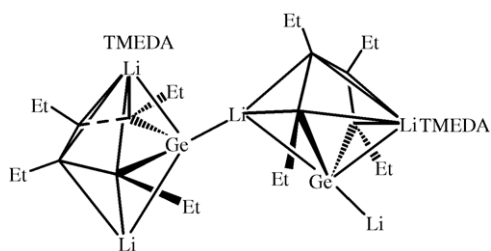


Fig. 11. X-ray structure of **46**.

**46**. Dianion **46** was isolated as colorless crystals from a saturated red THF/TMEDA solution and characterized by X-ray analysis. One lithium is  $\eta^5$ -coordinated to the  $\text{C}_4\text{Ge}$  ring and to TMEDA, while the other lithium is  $\eta^5$ -coordinated to the  $\text{C}_4\text{Ge}$  ring fragment and also  $\eta^1$ -coordinated to the germanium atom of another  $\text{C}_4\text{Ge}$  ring. This combination of linkages results in a polymeric network. It is noteworthy that the  $^7\text{Li}$  NMR spectrum of solutions of X-ray quality crystals of **46** showed a broad signal attributable to  $\pi$ -complexation at  $-5.63$  ppm [43]. The upfield resonance of the germole dianion in the  $^7\text{Li}$  NMR spectrum was also predicted by theoretical calculations [11].

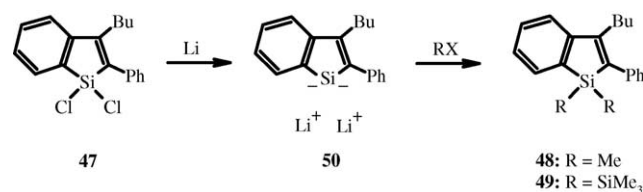
## 8. Synthesis and structures of benzannulated silole and germole dianions

### 8.1. Metallaindene dianions

Since the first report on the synthesis of silole dianion **30** in 1990, there has been a remarkable development in the investigation on the structures of silole and germole dianions. On the basis of crystal structure analyses, NMR studies, and theoretical calculations, they are believed to have an aromatic character with delocalized electrons and equalized C–C bond lengths. Attention has been subsequently paid to the effect of benzannulation of metallole dianions.

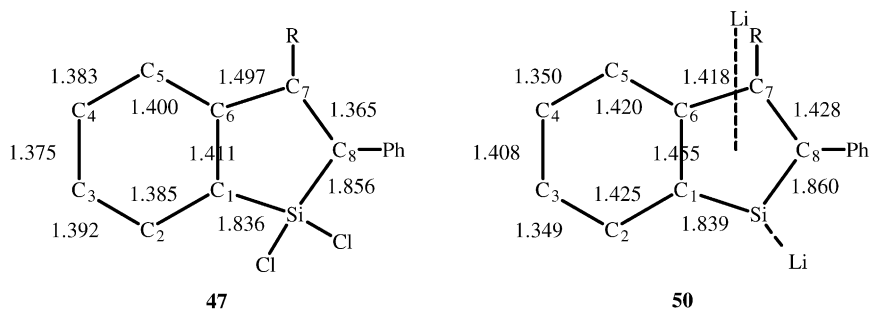
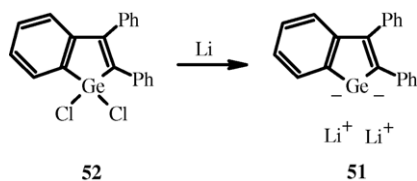
Reaction of 1,1-dichlorosilaindene **47** with lithium produced a dark-red solution, and treatment of this solution with methyl iodide or chlorotrimethylsilane gave 1,1-dimethyl **48** or 1,1-bis(trimethylsilyl)silaindene **49**, indicating the formation of intermediary silaindenyl dianion **50** (Scheme 13) [44]. Compound **50** was isolated as X-ray quality crystals and its structure was established by X-ray analysis. One lithium ion is  $\eta^1$ -coordinated to the silicon atom and also coordinated to three dioxane molecules, while the other is  $\eta^5$ -coordinated to the  $\text{SiC}_4$  ring fragment and also coordinated to two dioxane molecules. The C–C bond lengths in the silole ring and the six-membered ring in **47** and **50** are remarkably different (Fig. 12). The  $\text{C}_6$ – $\text{C}_7$  bond is significantly shortened and the  $\text{C}_1$ – $\text{C}_6$  and  $\text{C}_7$ – $\text{C}_8$  bond bonds are lengthened in **50**. Such changes in bond lengths indicate that the  $\text{SiC}_4$  ring has aromatic character and the six-membered ring has diene properties.

The  $^{29}\text{Si}$  NMR signal for **50** (29.19 ppm) is significantly downfield compared to that of **47** (5.92 ppm). This is due to effective  $\pi$ -delocalization in the silole ring.



Scheme 13.



Fig. 12. Selected bond lengths (angstroms) of **47** and **50**.

Scheme 14.

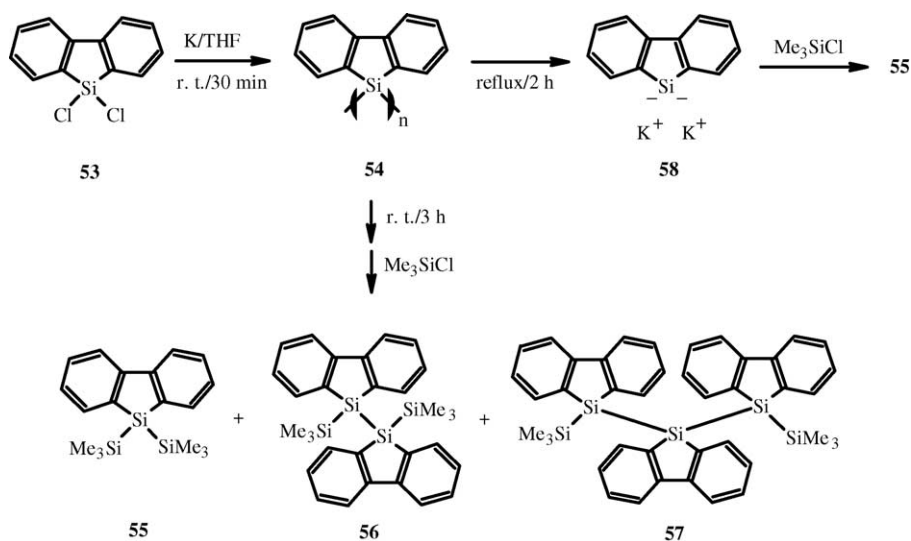
The  $^7\text{Li}$  NMR spectrum of a solution of **50** showed only one signal at  $-0.20$  ppm over the temperature range of  $25$  to  $-40^\circ\text{C}$ . These data, as in the case of tetraphenylsilole dianion **31** [37], suggest the rapid exchange of the  $\eta^1$ - and  $\eta^5$ -lithium cations probably due to presence of  $\text{LiCl}$  and hence the structure of **50** in solution is still ambiguous.

Germainene dianion **51** was also synthesized by the reduction of the corresponding 1,1-dichloro derivative **52** with lithium (Scheme 14) [45]. X-ray analysis of germainene dianion **51** shows the  $\text{GeC}_4$  ring with aromatic character and the six-membered ring with diene properties, as in the case of silaindene dianion **50** [44].

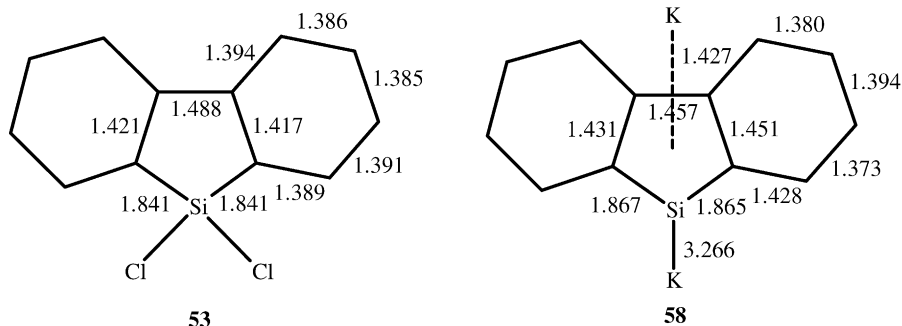
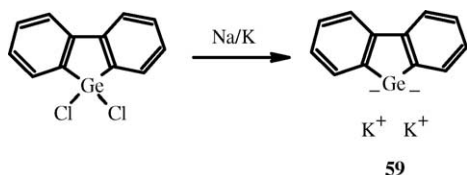
## 8.2. Metallafluorene dianions

After the first report on the synthesis of a silafluorene dianion [46], a number of works on the synthesis and structural analysis of a silafluorene dianion were published [47]. Reaction of 1,1-dichlorosilafluorene **53** with potassium in THF led to an insoluble white solid, probably a polysilafluorene **54** (Scheme 15). Further reaction with potassium to cleave the Si–Si bonds in **54** followed by treatment with chlorotrimethylsilane gave a mixture of trisilane **55**, tetrasilane **56**, and pentasilane **57**, suggesting the formation of the silafluorene dianion **58**. Complete cleavage of the Si–Si bonds in **54** requires 2 h of refluxing. In fact, trapping of the reaction mixture after refluxing for 2 h with chlorotrimethylsilane gave **55** exclusively.

X-ray quality crystals of **58** were obtained by crystallization from DME/hexane in the presence of 18-crown-6. One of two potassium atoms is  $\eta^5$ -bonded to the silole ring and the other is  $\eta^1$ -bonded to the silicon atom (Fig. 13). The same arrangement of the alkali metals was found in silole **31** [37] and silaindene dianions **50** [44]. The five-membered ring has nearly equal C–C bond lengths and an  $\eta^5$ -bonded potassium locates above the ring. Thus, the lone pair electrons



Scheme 15.

Fig. 13. Selected bond lengths (angstroms) of **53** and **58**.

Scheme 16.

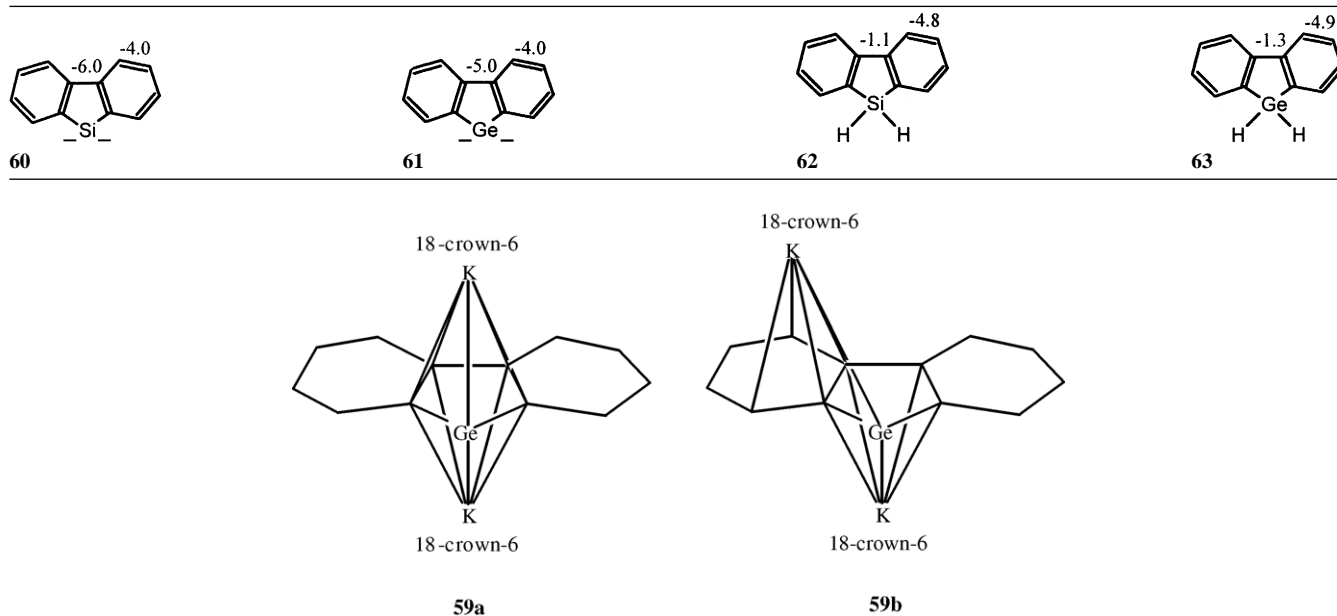
in the silafluorene dianion **58** are highly delocalized. Bond alternation occurs in the two six-membered benzene rings. Moreover, the aromatic delocalization in the silole ring takes precedence over that in the benzenoid rings. The short distance of  $\eta^1$ -bonded Si–K (3.266 Å) suggests the localization of the second lone pair of electrons on the silicon atom.

The germafluorene dianion was also synthesized by the reduction of the corresponding dichloride with Na/K alloy (Scheme 16) [48]. In the presence of 18-crown-6, two types of deep-green crystals were formed (Fig. 14). The first

has two potassium atoms  $\eta^5$ -coordinated to the central five-membered ring, as depicted by **59a**, and the second type has a potassium atom  $\eta^5$ -bonded to the germole ring and a potassium atom coordinated mainly to the germafluorene ring, as depicted by **59b**. The C–C bond distances of the five-membered ring in both **59a** and **59b** are nearly equal, so that the negative charges are considerably delocalized in the germole ring. On the other hand, bond alternation occurs in the six-membered ring. The aromatic delocalization into the germole ring would take precedence over that in the benzenoid rings, as was found in **58**.

NICS is known to be an effective probe of the individual rings in polycyclic system [29,49,50]. The NICS values of sila- and germafluorene dianions **60** and **61** as well as the sila- and germafluorene **62** and **63** with the ghost atom located 2.0 Å above the ring centroid [NICS(2.0)] [51] were calculated (Table 2). The five-membered rings in dianions **60** and **61** have more negative NICS values than the six-

Table 2  
NICS(2.0) Values of sila- and germafluorene dianions

Fig. 14. X-ray structures of **59**.

membered benzenoid rings so that the five-membered ring has greater aromatic character than the six-membered ring, whereas the corresponding neutral fluorenes **62** and **63** have more negative NICS value in the six-membered ring than in the five-membered ring. The five-membered rings in **62** and **63** are less aromatic than the six-membered rings.

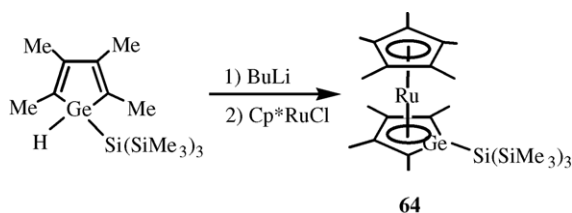
## 9. $\eta^5$ -Sila- and germacyclopentadienyl transition metal complexes

### 9.1. Synthesis, structures, and properties

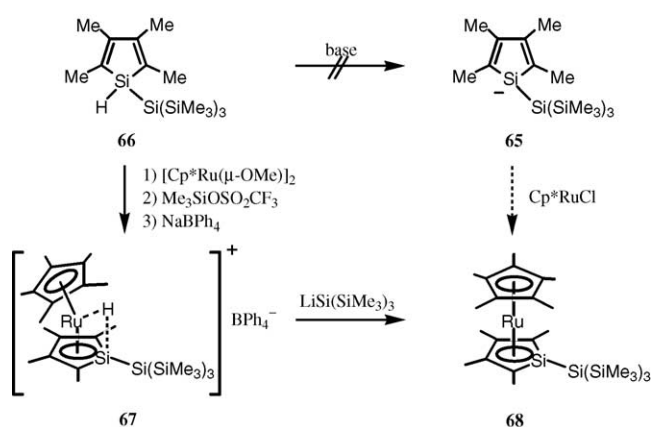
The  $\eta^5$ -sila- and  $\eta^5$ -germacyclopentadienyl transition metal complexes are fascinating synthetic targets as heavier congeners of ferrocene, which has played an important role in organometallic chemistry for five decades. After numerous unsuccessful attempts for the syntheses of such species [5a], the first isolation of  $\eta^5$ -germacyclopentadienyl ruthenium complex **64** was reported in 1993 (Scheme 17) [52].

The  $^{13}\text{C}$  NMR spectrum of **64** showed two signals assignable to the germole ring carbon centers at 80.23 and 87.82 ppm and a signal assignable to the  $\text{Cp}^*$  ring carbon centers at 85.38 ppm. X-ray analysis of **64** showed two planar five-membered rings coordinated in a sandwich fashion to the ruthenium atom. Because of the  $\text{sp}^2$  hybridization of the germanium atom, the germanium atom deviates by only 0.02 Å from the germole ring's least-squares plane. The sum of angles around the germanium atom is 358.1°, and the endocyclic C–C bond lengths are almost equal. Interestingly, **64** demonstrated an irreversible oxidation wave at  $E_{1/2} = 0.25$  V (versus SCE) by cyclic voltametry, while decamethylruthenocene displayed a reversible oxidation wave at  $E_{1/2} = 0.42$  V under comparable conditions [53]. Such electrochemical data suggest that the germole ligand and  $\eta^5$ - $\text{C}_4\text{Me}_4\text{Ge}$  is more electron-donating than  $\eta^5$ - $\text{C}_5\text{Me}_5$ .

The synthesis of  $\eta^5$ -silacyclopentadienyl transition metal complexes was also attempted [54]. Although initial attempts through the generation of silole anion **65** by the reaction of the corresponding silyl analog **66** with a base such as  $\text{KN}(\text{SiMe}_3)_2$ ,  $(\text{THF})_3\text{LiSi}(\text{SiMe}_3)_2$ , or  $\text{KH}/18\text{-crown-6}$  failed, direct synthesis from **66** with  $\text{Cp}^*\text{Ru}^+$  and  $\text{NaBPh}_4$  gave a cationic  $\pi$ -complex **67**, as shown in Scheme 18. The  $^1\text{H}$  NMR spectrum of **67** showed an upfield signal at  $-8.82$  ppm assignable to the metal hydride on ruthenium with  $^1J(\text{Si}-\text{H})$  of 41 Hz. X-ray analysis of **67** showed the planar  $\text{C}_4\text{Si}$  ring with the sum of angles around Si of 355.1° and a small difference between the endocyclic C–C bonds of 0.07 Å.



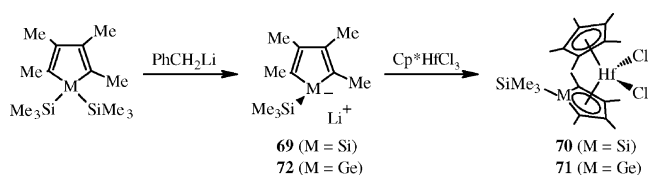
Scheme 17.



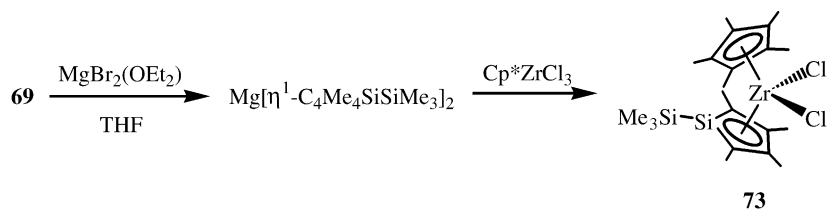
Scheme 18.

Deprotonation of **67** is a straightforward method for the synthesis of the desired complex **68**. Reaction of **67** with  $(\text{THF})_3\text{LiSi}(\text{SiMe}_3)_3$  gave **68** and  $\text{Si}(\text{SiMe}_3)_4$  (Scheme 18). The compound  $\text{Si}(\text{SiMe}_3)_4$  may arise from a secondary reaction of  $(\text{THF})_3\text{LiSi}(\text{SiMe}_3)_3$  with the initially formed deprotonation product  $\text{HSi}(\text{SiMe}_3)_3$  [55]. The  $^1\text{H}$  and  $^{13}\text{C}$  NMR spectra of **68** closely resembled those of **64**.

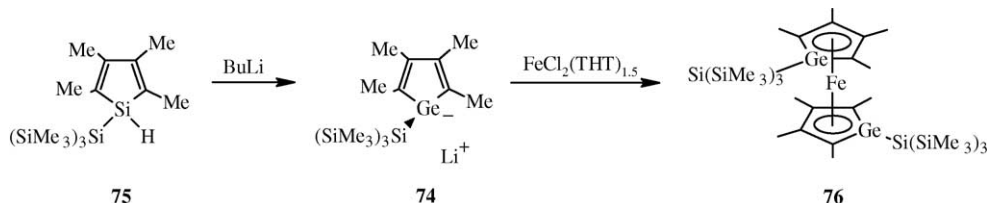
Four years after the synthesis of **68**, the synthesis and structural characterization of  $\eta^5$ -silacyclopentadienyl transition metal complexes were reported [56]. Among the reported silole anions, the lithium derivative **69** bearing a trimethylsilyl group on silicon was used for the preparation of transition metal complexes. Although the reaction of **69** with  $\text{ZrCl}_4$ ,  $\text{HfCl}_4$ ,  $\text{CpTiCl}_3$ , and  $\text{Cp}^*\text{TiCl}_3$  did not afford any isolable products, the reaction with  $\text{Cp}^*\text{HfCl}_3$  produced the bent  $\eta^5$ -silacyclopentadienyl complex **70** (Scheme 19). The molecular structure of **70** consists of two planar five-membered rings coordinated in a bent fashion to hafnium. The silole ring has nearly planar geometry as evidenced by the sum of angles around Si (354.7°). The compound **70** has longer  $\text{C}_\alpha\text{--C}_\beta$  bonds (1.42(1) and 1.46(2) Å) than  $\text{C}_\beta\text{--C}_\beta$  bond (1.37(2) Å), whereas siloles and silole anions have longer  $\text{C}_\beta\text{--C}_\beta$  bonds than  $\text{C}_\alpha\text{--C}_\beta$  bonds [16,26,38,52,54]. Thus, the  $\text{C}_4$  fragment in **70** probably  $\sigma^2$ ,  $\pi$ -coordinates to hafnium. The  $^{29}\text{Si}$  NMR resonance for the ring Si atom in **70** appears significantly downfield (49.7 ppm) from that in **18** ( $-41.52$  ppm), strongly suggesting the participation of Si in  $\pi$ -delocalization. The germole complex **71** was also synthesized by the reaction of germole anion **72** with  $\text{Cp}^*\text{HfCl}_3$  and characterized by X-ray analysis (Scheme 19).



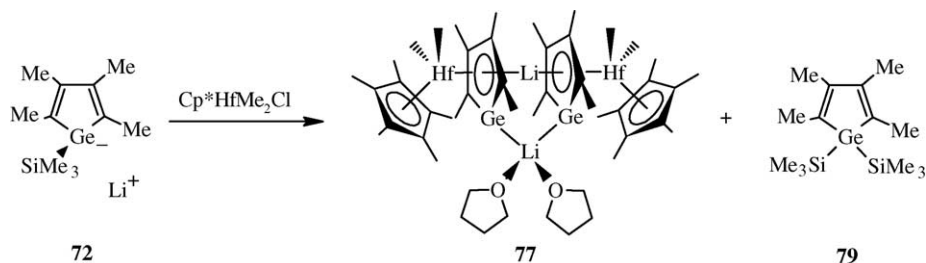
Scheme 19.



Scheme 20.



Scheme 21.



Scheme 22.

The zirconium complex of a silole anion **73** was also synthesized in a manner similar to the synthesis of **70** and **71** (Scheme 20) [57]. The  $\sigma^2$ ,  $\pi$ -coordination of the  $C_4$  fragment to zirconium was established by X-ray crystallographic analysis.

Very recently, the germacyclopentadienyl complex of iron, a heavier congener of ferrocene, was successfully synthesized and characterized [58]. Reaction of **74** (2 eq) generated from the treatment of **75** with butyllithium with  $\text{FeCl}_2(\text{THT})_{1.5}$  (THT = tetrahydrothiophene) resulted in the formation of a deep-red solution from which a germanium analog of ferrocene **76** was isolated (Scheme 21). X-ray analysis of **76** showed two coplanar  $\eta^5$ -germoly rings bound in a sandwich fashion to the iron center. The bulky tris(trimethylsilyl)silyl group on the germanium atom is necessary for the formation of the digermaferrocene complexes. A similar reaction with other germole anions did not afford digermaferrocene complexes cleanly.

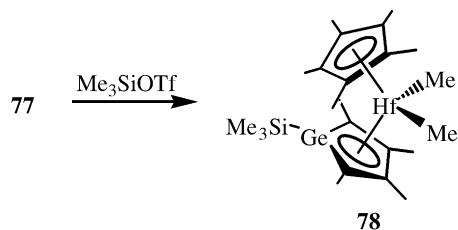
The germole dianion complex was obtained by the reaction of the germole dianion with the hafnium complex [57]. Reaction of  $\text{Cp}^*\text{HfMe}_2\text{Cl}$  with germole dianion **72** gave germole dianion complex **77** in high yield together with 1,1-bis(trimethylsilyl)germole **79** (Scheme 22). The reaction of **72** with  $\text{Cp}^*\text{HfMe}_2\text{Cl}$  is believed to proceed with a faster loss of chlorotrimethylsilane (which reacts with **72** to afford **79**) than the elimination of  $\text{LiCl}$  to give the anticipated metallocene derivative  $\text{Cp}^*[\eta^5\text{-C}_4\text{Me}_4\text{GeSiMe}_3]\text{HfMe}_2$  **78**. X-ray

analysis showed that compound **77** was a dimer of  $\text{Li}[\text{Cp}^*(\eta^5\text{-C}_4\text{Me}_4\text{GeSiMe}_3)\text{HfMe}_2]$  in which the germole dianion rings were bridged by two lithium atoms. One lithium atom is sandwiched in an  $\eta^5$ -fashion between the two germole rings, while the other lithium atom is coordinated in an  $\eta^1$ -fashion by both germanium atoms.

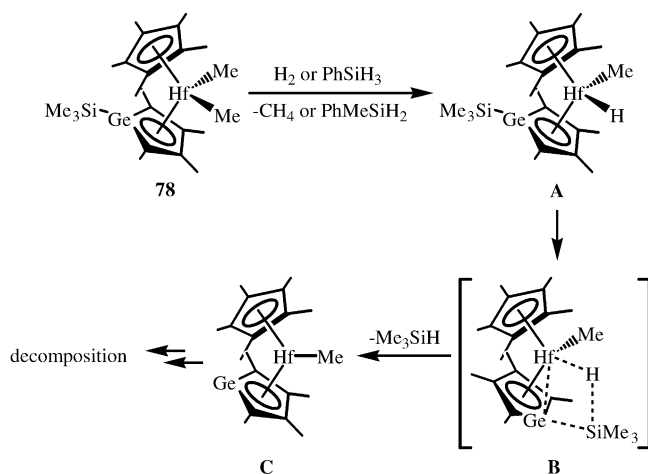
## 9.2. Reactivity

Recently, much attention has been devoted to the use of cationic group 4 bent metallocene complexes for the polymerization of olefins [59]. These complexes are formed upon abstraction of a methyl anion from the group 4 metal center.  $\text{Cp}^*[\eta^5\text{-C}_4\text{Me}_4\text{GeSiMe}_3]\text{HfMe}_2$  **78** is a good compound for this purpose and is produced by the reaction of **77** with  $\text{Me}_3\text{SiOTf}$  (Scheme 23) [57].

The hafnium–methyl bonds in **78** are active toward  $\sigma$ -bond metathesis. Exposure of **78** to an excess of  $\text{H}_2$  at



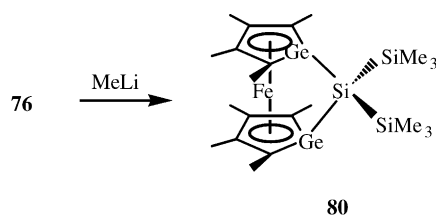
Scheme 23.



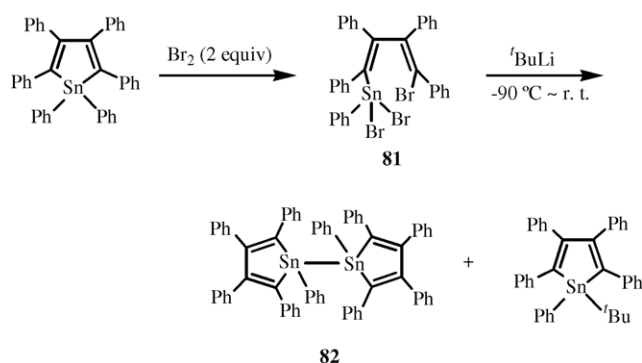
Scheme 24.

25 °C resulted in the formation of CH<sub>4</sub> (1 equiv) and Me<sub>3</sub>SiH (0.4 equiv). Likewise, the reaction of **78** with PhSiH<sub>3</sub> gave PhMeSiH<sub>2</sub> (1.0 equiv) and Me<sub>3</sub>SiH (0.63 equiv), along with an unidentifiable organometallic species (Scheme 24). It is noted that the CpCp\*HfMe<sub>2</sub> complex does not react with PhSiH<sub>3</sub> at room temperature over several weeks [60], while Cp<sub>2</sub>ZrMe<sub>2</sub> requires more than 86 h to completely react with H<sub>2</sub> at 1 atm at room temperature [61], and Cp\*<sub>2</sub>ZrMe<sub>2</sub> reacts with H<sub>2</sub> at 1 atm to give the corresponding dihydride only after heating to 70 °C for 1 week [62]. Thus, the germolyl ring in **78** significantly enhances the reactivity of the hafnium–methyl bonds. The initial step of the reaction of **78** with H<sub>2</sub> or PhSiH<sub>3</sub> may be the formation of a hafnium hydride (**A**) via  $\sigma$ -bond metathesis with H<sub>2</sub> or PhSiH<sub>3</sub>. The Me<sub>3</sub>SiH appears to form through the abstraction of the hydride ligand by the germole-bound –SiMe<sub>3</sub> group (**B**). However, attempts to trap the neutral germole dianion complex **C** with various reagents failed.

It has been known that silicon-bridged ferrocenophanes are very good precursors for the preparation of high molecular weight polyferrocene [63]. This chemistry relies on the high ring strain in metallocenophane monomers that possess a single silicon atom bridge between the two cyclopentadienyl ligands. As a precursor to iron-germolyl-containing polymers, the silicon-bridged germaferrocenophane was synthesized and characterized [58]. Reaction of **76** with methyl-lithium gave the silicon-bridged germaferrocenophane **80** (Scheme 25). Thermolysis of solid **80** up to 260 °C, however, did not give any polymeric materials with the recovery of un-



Scheme 25.



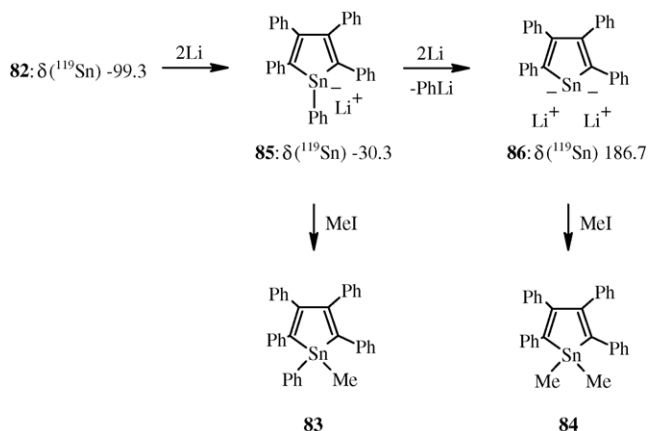
Scheme 26.

reacted **80**. The anionic polymerization initiated by PhCH<sub>2</sub>Li or BuLi likewise gave no polymeric materials.

## 10. Synthesis and reactions of stannole anions and dianions

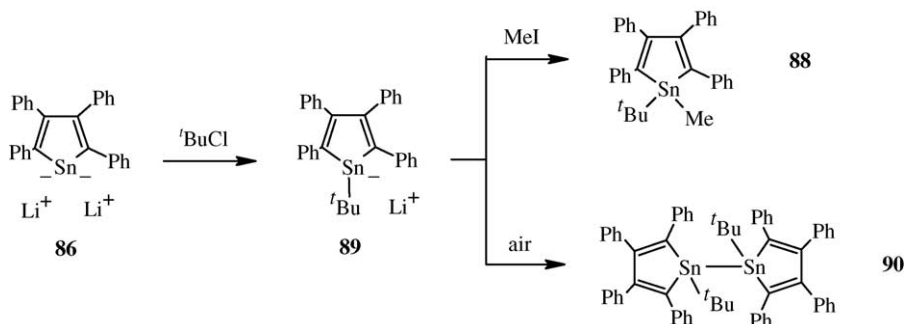
In contrast to the well-investigated mono- and dianions of siloles and germoles, neither mono- nor dianions of stannole had been reported before our project to investigate stannole mono- and dianions, although they are fascinating synthetic targets in terms of potential tin-containing aromatic compounds. The 1,1-dihalogenated stannoles are expected to be good precursors to anionic species of the stannole. Zuckerman et al. reported that the reaction of 1,1-diphenylstannoles with halogens gave 1,1-dihalostannoles [64]. We tried to prepare 1,1-dihalostannoles by Zuckerman's method. However, the reaction of 1,1,2,3,4,5-hexaphenylstannole with bromine gave the ring-opened halogenated products **81** instead of the 1,1-dihalostannoles (Scheme 26) [65]. Compound **81** underwent debrominative cyclization to give bi(1,1-stannole) **82** which was expected to be a good precursor to a stannole monoanion [66].

Treatment of **82** with excess lithium in THF at room temperature gave a dark-red solution. By the addition of methyl iodide to this solution, 1-methyl-1-phenylstannole **83** was ob-



Scheme 27.





Scheme 28.

tained as a major product together with 1,1-dimethylstannole **84**. Thus, the reduction of **82** by lithium revealed the evidence not only for the formation of the stannole monoanion **85** but also for the formation of the stannole dianion **86** (Scheme 27). The exhaustive reduction of **82** by refluxing a THF solution of **82** in the presence of excess lithium followed by treatment of the reaction mixture with methyl iodide afforded 1,1-dimethylstannole **84** as a main product. The stannole dianion **86** was probably formed by the reductive cleavage of the Sn–phenyl bond in the initially formed **85**. Reductive cleavage of the Si–phenyl bond of 1-phenylsilole anion with lithium also occurred to give silole dianion **31** with the formation of phenyllithium [67].

The  $^{119}\text{Sn}$  NMR signal attributable to stannole monoanion **85** (−30.3 ppm) appeared in lower field than that for **82** (−99.3 ppm in  $\text{CDCl}_3$ ). A possible interpretation of the downfield shift of **85** compared to **82** in the  $^{119}\text{Sn}$  NMR may be a partial delocalization of the negative charge in the ring, as was observed in silole anion **16** [12]. After the reduction of **85** proceeded, only one new signal assignable to stannole dianion **86** was observed at 186.7 ppm. The remarkable downfield shift of the  $^{119}\text{Sn}$  signal for **86** is reasonably interpreted in terms of strong participation of a resonance form with stannylene character (Plate 5), as was observed in silole dianion **31** showing silylene character (Plate 4) [32]. The central tin of the isolobal diaminostannylene **87** is known to resonate at 237 ppm [68]. In  $^{13}\text{C}$  NMR, the signal with large  $^nJ(\text{Sn}-^{13}\text{C})$  of about 320 Hz assignable to  $\alpha$ -carbon in the five-membered ring of **86** was observed at 184.58 ppm. The remarkable downfield resonance of the  $\alpha$ -carbon in silole dianion was also predicted by calculation [28].

The alkylation of **86** was studied to synthesize a stannole anion from the dianion **86** [69]. When *t*-butyl chloride was

added to an ether solution of **86** at room temperature, the color of the solution turned from deep red to bright red. By the treatment of the reaction mixture with methyl iodide, 1-*t*-butyl-1-methylstannole **88** was obtained suggesting the formation of stannole anion **89** by alkylation of **86** (Scheme 28). The formation of **89** from **86** was reasonably explained in terms of an electron transfer mechanism in analogy with the reaction of a tributylstannyl anion with *t*-butyl halides [70]. The reaction of **86** with *t*-butyl chloride followed by exposure of the reaction mixture to air without treatment of methyl iodide gave bi(1,1-stannole) **90** (Scheme 28). Since the silyl anion is known to be oxidized by  $\text{NO}^+$  to a silyl radical [71], the formation of **90** is reasonably interpreted in terms of dimerization of the 1-*t*-butylstannole radical resulting from air oxidation of **89**.

## 11. Conclusion

Synthesis and Properties of group 14 metallole anions and dianions have been discussed. The negative charge in the C-phenylated metallole anions is partially delocalized in the ring, while that in the C-alkylated metallole anions localizes on the metal. The metallole dianions have delocalized negative charge in the ring and show considerable aromatic character as evidenced by NMR studies, X-ray structural analysis and theoretical calculations. Metallylene is a major contributor in metallole dianions. In benzannulated metallole dianions, the negative charge is more localized in the metallole ring than in the benzenoid rings. Silole and germole anions and dianions can be used for the synthesis of  $\eta^5$ -silolyl and  $\eta^5$ -germolyl metal complexes, analogs of ferrocene. These complexes have unique reactivity based on the activation of the metal–carbon bond toward  $\sigma$ -bond metathesis.

## Acknowledgments

Our work described in this review was partially supported by Grants-in-Aid for Young Scientists (B), Nos. 10740288 (M. S.) and 13740349 (M. S.) from the Ministry of Education, Culture, Sports, Science and Technology, Japan and from Japan Society for the Promotion of Science, respectively. M. Saito also acknowledges a research grant for young

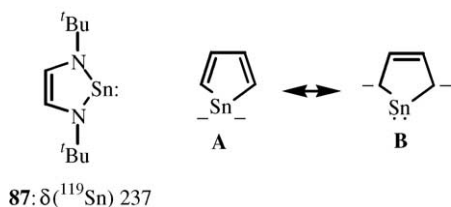


Plate 5.

scientists from Nissan Science Foundation, Sasakawa Scientific Research Grant from The Japan Science Society, and a research grant from Toray Science Foundation.

## References

- [1] (a) D.E. Goldberg, D.H. Harris, M.F. Lappert, K.M. Thomas, *Chem. Commun.* (1976) 261;  
(b) P.J. Davidson, D.H. Harris, M.F. Lappert, *J. Chem. Soc., Dalton Trans.* (1976) 2268.
- [2] R. West, M. Fink, J. Michl, *Science* 214 (1981) 1343.
- [3] (a) M. Yoshifuji, I. Shima, N. Inamoto, K. Hirotsu, T. Higuchi, *J. Am. Chem. Soc.* 103 (1981) 4587;  
(b) M. Yoshifuji, I. Shima, N. Inamoto, K. Hirotsu, T. Higuchi, *J. Am. Chem. Soc.* 104 (1982) 6167.
- [4] (a) J. Satgé, *Pure Appl. Chem.* 56 (1984) 137;  
(b) R. West, *Pure Appl. Chem.* 56 (1984) 163;  
(c) G. Raabe, J. Michl, *Chem. Rev.* 85 (1985) 419;  
(d) A.G. Brook, K.M. Baines, *Adv. Organomet. Chem.* 25 (1986) 1;  
(e) R. West, *Angew. Chem., Int. Ed.* 26 (1987) 1201;  
(f) G. Raabe, J. Michl, *The Chemistry of Organosilicon Compounds*, Wiley-Interscience, Chichester, 1989;  
(g) J. Barrau, J. Escudié, J. Satgé, *Chem. Rev.* 90 (1990) 283;  
(h) J. Satgé, *J. Organomet. Chem.* 400 (1990) 121;  
(i) T. Tsumuraya, S.A. Batcheller, S. Masamune, *Angew. Chem., Int. Ed.* 30 (1991) 902;  
(j) A.G. Brook, M.A. Brook, *Adv. Organomet. Chem.* 39 (1996) 71;  
(k) M. Driess, *Adv. Organomet. Chem.* 39 (1996) 193;  
(l) R. Okazaki, R. West, *Adv. Organomet. Chem.* 39 (1996) 232;  
(m) K.M. Baines, W.G. Stibbs, *Adv. Organomet. Chem.* 39 (1996) 275;  
(n) P.P. Power, *J. Chem. Soc., Dalton. Trans.* (1998) 2939;  
(o) T. Müller, W. Ziche, N. Auner, in: S. Patai, Z. Rappoport (Eds.), *The Chemistry of Organosilicon Compounds*, vol. 2, Wiley-Interscience, Chichester, 1998, p. 857;  
(p) N. Tokitoh, R. Okazaki, in: S. Patai, Z. Rappoport (Eds.), *The Chemistry of Organosilicon Compounds*, vol. 2, Wiley-Interscience, Chichester, 1998, p. 1063;  
(q) R. Okazaki, N. Tokitoh, *Acc. Chem. Res.* 33 (2000) 625;  
(r) N. Takeda, N. Tokitoh, R. Okazaki, *Science of syntheses*, in: M.G. Moloney (Ed.), *Houben-Weyl Methods of Molecular Transformations*, vol. 5, George Thieme Verlag, Stuttgart, 2002, p. 27;  
(s) N. Takeda, N. Tokitoh, R. Okazaki, *Science of syntheses*, in: M.G. Moloney (Ed.), *Houben-Weyl Methods of Molecular Transformations*, vol. 5, George Thieme Verlag, Stuttgart, 2002, p. 299;  
(t) N. Takeda, N. Tokitoh, R. Okazaki, *Science of syntheses*, in: M.G. Moloney (Ed.), *Houben-Weyl Methods of Molecular Transformations*, vol. 5, George Thieme Verlag, Stuttgart, 2002, p. 637.
- [5] (a) E. Colomer, R.J.P. Corriu, M. Lheureux, *Chem. Rev.* 90 (1990) 265;  
(b) J. Dubac, C. Guérin, P. Meunier, in: S. Patai, Z. Rappoport (Eds.), *The Chemistry of Organosilicon Compounds*, vol. 2, Wiley-Interscience, Chichester, 1998, p. 1961.
- [6] H. Gilman, R.D. Gorsich, *J. Am. Chem. Soc.* 80 (1958) 3243.
- [7] M.D. Curtis, *J. Am. Chem. Soc.* 89 (1967) 4241.
- [8] B. Goldfuss, P.v.R. Schleyer, *Organometallics* 14 (1995) 1553.
- [9] Julg's parameter (*A*) defines the degree of aromaticity in terms of deviations of (*n*) individual C–C bond lengths (*r<sub>i</sub>*) from the mean carbon bond length (*r*): *A* = 1 for benzene (*D<sub>6h</sub>*) and *A* = 0 for Kekulé benzene (*D<sub>3h</sub>*), assuming C–C distances of 1.33 and 1.52 Å. *A* = 1 – (225/*n*)∑(1–*r<sub>i</sub>*/*r*)<sup>2</sup>, see ref. 10.
- [10] (a) A. Julg, P. Francois, *Theor. Chim. Acta* 7 (1967) 249;  
(b) S.M.v.d. Kerk, *J. Organomet. Chem.* 215 (1981) 315.
- [11] B. Goldfuss, P.v.R. Schleyer, *Organometallics* 16 (1997) 1543.
- [12] J.-H. Hong, P. Boudjouk, *J. Am. Chem. Soc.* 115 (1993) 5883.
- [13] (a) G.A. Olah, R.J. Hunadi, *J. Am. Chem. Soc.* 102 (1980) 6989;  
(b) H. Söllradl, E. Hengge, *J. Organomet. Chem.* 243 (1983) 257.
- [14] F. Mathey, *Chem. Rev.* 88 (1988) 429, references cited therein.
- [15] W.P. Freeman, T. Don Tilley, G.P.A. Yap, A.L. Rheingold, *Angew. Chem., Int. Ed.* 35 (1996) 882.
- [16] W.P. Freeman, T. Don Tilley, L.M. Liable-Sands, A.L. Rheingold, *J. Am. Chem. Soc.* 118 (1996) 10457.
- [17] (a) R.L. Scholl, G.E. Maciel, W.K. Musker, *J. Am. Chem. Soc.* 94 (1972) 6376;  
(b) K.G. Sharp, P.A. Sutor, E.A. Williams, J.D. Cargioli, T.C. Farrar, K. Ishibitsu, *J. Am. Chem. Soc.* 98 (1976) 1977;  
(c) D.A. Stanislawski, R. West, *J. Organomet. Chem.* 204 (1981) 295;  
(d) A. Sekiguchi, M. Nanjo, C. Kabuto, H. Sakurai, *Organometallics* 14 (1995) 2630.
- [18] J. March, *Advanced Organic Chemistry*, fourth ed., Wiley, New York, 1992.
- [19] J.-H. Hong, P. Boudjouk, I. Stoescu, *Organometallics* 15 (1996) 2179.
- [20] (a) U. Edlund, T. Lejon, T.K. Venkatachalam, E. Buncel, *J. Am. Chem. Soc.* 107 (1985) 6408;  
(b) U. Edlund, T. Lejon, P. Pyykkö, T.K. Venkatachalam, E. Buncel, *J. Am. Chem. Soc.* 109 (1987) 5982.
- [21] (a) E. Buncel, T.K. Venkatachalam, B.J. Eliasson, U. Edlund, *J. Am. Chem. Soc.* 107 (1985) 303;  
(b) E. Buncel, T. K. Venkatachalam, U. Edlund, B.J. Eliasson, *Chem. Commun.* (1984) 1476.
- [22] S.-B. Choi, P. Boudjouk, *J. Chem. Soc., Dalton Trans.* (2000) 841.
- [23] P. Jutz, A. Karl, *J. Organomet. Chem.* 215 (1981) 19.
- [24] P. Dufour, J. Dubac, M. Dartiguenave, Y. Dartiguenave, *Organometallics* 9 (1990) 3001.
- [25] (a) R.J. Batchelor, T. Birchall, *J. Am. Chem. Soc.* 105 (1983) 3848;  
(b) A. Castel, P. Rivière, J. Satgé, Y.-H. Ko, *J. Organomet. Chem.* 342 (1988) C1;  
(c) A. Castel, P. Rivière, J. Satgé, Y.-H. Ko, *Organometallics* 9 (1990) 205.
- [26] W.P. Freeman, T. Don Tilley, F.P. Arnold, A.L. Rheingold, P.K. Gantzel, *Angew. Chem., Int. Ed.* 34 (1995) 1887.
- [27] W. Kutzelnigg, *Angew. Chem., Int. Ed.* 23 (1984) 272.
- [28] B. Goldfuss, P.v.R. Schleyer, F. Hampel, *Organometallics* 15 (1996) 1755.
- [29] P.v.R. Schleyer, C. Maerker, A. Dransfeld, H. Jiao, N.J.R.v.E. Hommes, *J. Am. Chem. Soc.* 118 (1996) 6317.
- [30] (a) L.A. Paquette, W. Bauer, M.R. Sivik, M. Bühl, M. Feigel, P.v.R. Schleyer, *J. Am. Chem. Soc.* 112 (1990) 8776;  
(b) H. Jiao, P.v.R. Schleyer, *Angew. Chem., Int. Ed.* 32 (1993) 1760.
- [31] W.-C. Joo, J.-H. Hong, S.-B. Choi, H.-E. Son, C.H. Kim, *J. Organomet. Chem.* 391 (1990) 27.
- [32] J.-H. Hong, P. Boudjouk, S. Castellino, *Organometallics* 13 (1994) 3387.
- [33] J.B. Stothers, *Carbon-13 NMR Spectroscopy*, Academic Press, New York, 1972.
- [34] (a) F. Mathey, *Top. Phosphorus Chem.* 10 (1980) 1;  
(b) C. Charrier, N. Maigrot, F. Mathey, *Organometallics* 6 (1987) 586.
- [35] N.M. Kostic, R.F. Fenske, *Organometallics* 2 (1983) 1008.
- [36] (a) M. Denk, R. K. Hayashi, R. West, *Chem. Commun.* (1994) 33;  
(b) M. Denk, R. Lennon, R.K. Hayashi, R. West, A.V. Belyakov, H.P. Verne, A. Haaland, M. Wagner, N. Metzler, *J. Am. Chem. Soc.* 116 (1994) 2691.
- [37] R. West, H. Sohn, U. Bankwitz, J. Calabrese, Y. Apeloig, T. Mueller, *J. Am. Chem. Soc.* 117 (1995) 11608.
- [38] U. Bankwitz, H. Sohn, D.R. Powell, R. West, *J. Organomet. Chem.* 499 (1995) 7.
- [39] J.-H. Hong, P. Boudjouk, *Bull. Soc. Chim. Fr.* 132 (1995) 495.

- [40] S.N. Tandura, S.P. Kolesnikov, K.S. Nosov, M.P. Egorov, O.M. Nefedov, *Main Group Met. Chem.* 22 (1999) 9.
- [41] R. West, H. Sohn, D.R. Powell, T. Müller, Y. Apeloig, *Angew. Chem., Int. Ed.* 35 (1996) 1002.
- [42] S.-B. Choi, P. Boudjouk, J.-H. Hong, *Organometallics* 18 (1999) 2919.
- [43] H. Sakurai, *Pure Appl. Chem.* 66 (1994) 1431.
- [44] S.-B. Choi, P. Boudjouk, P. Wei, *J. Am. Chem. Soc.* 120 (1998) 5814.
- [45] S.-B. Choi, P. Boudjouk, K. Qin, *Organometallics* 19 (2000) 1806.
- [46] S.-B. Choi, P. Boudjouk, *Tetrahedron. Lett.* 41 (2000) 6685.
- [47] Y. Liu, T.C. Stringfellow, D. Ballweg, I.A. Guzei, R. West, *J. Am. Chem. Soc.* 124 (2002) 49.
- [48] Y. Liu, D. Ballweg, T. Müller, I.A. Guzei, R.W. Clark, R. West, *J. Am. Chem. Soc.* 124 (2002) 12174.
- [49] H. Jiao, P.v.R. Schleyer, Y. Mo, M.A. Mcallister, T.T. Tidwell, *J. Am. Chem. Soc.* 119 (1997) 7075.
- [50] H. Jiao, P.v.R. Schleyer, *Angew. Chem., Int. Ed.* 35 (1996) 2383.
- [51] P.v.R. Schleyer, H. Jiao, N.J.R.v.E. Hommes, V.G. Malkin, O.L. Malkina, *J. Am. Chem. Soc.* 119 (1997) 12669.
- [52] W.P. Freeman, T. Don Tilley, A.L. Rheingold, R.L. Ostrander, *Angew. Chem., Int. Ed.* 32 (1993) 1744.
- [53] P.G. Gassman, C.H. Winter, *J. Am. Chem. Soc.* 110 (1988) 2310.
- [54] W.P. Freeman, T. Don Tilley, A.L. Rheingold, *J. Am. Chem. Soc.* 116 (1994) 8428.
- [55] H. Gilman, C.L. Smith, *J. Organomet. Chem.* 14 (1968) 91.
- [56] J.M. Dysard, T. Don Tilley, *J. Am. Chem. Soc.* 120 (1998) 8245.
- [57] J.M. Dysard, T. Don Tilley, *J. Am. Chem. Soc.* 122 (2000) 3097.
- [58] W.P. Freeman, J.M. Dysard, T. Don Tilley, A.L. Rheingold, *Organometallics* 21 (2002) 1734.
- [59] (a) L. Jia, X.M. Yang, C.L. Stern, T.J. Marks, *Organometallics* 16 (1997) 842;  
(b) M. Bochmann, *J. Chem. Soc., Dalton Trans.* (1996) 225;  
(c) R.C. Mohring, N.J. Coville, *J. Organomet. Chem.* 479 (1994) 1;  
(d) T.J. Marks, *Acc. Chem. Res.* 25 (1992) 57.
- [60] C. Aitken, J.-P. Barry, F. Gauvin, J.F. Harrod, A. Malek, D. Rousseau, *Organometallics* 8 (1989) 1732.
- [61] R.F. Jordan, C.S. Bajgur, W.E. Dasher, A.L. Rheingold, *Organometallics* 6 (1987) 1041.
- [62] L.E. Scheck, T.J. Marks, *J. Am. Chem. Soc.* 110 (1988) 7701.
- [63] For a recent review of the polymerization of silicon-bridged ferrocenophanes, see: P. Nguyen, P. Gómez-Elipe, I. Manners, *Chem. Rev.* 99 (1999) 1515.
- [64] (a) W.Z.M. Rhee, J.J. Zuckerman, *J. Am. Chem. Soc.* 97 (1975) 2291;  
(b) W.A. Gustavson, L.M. Principe, W.-Z. Min Rhee, J.J. Zuckerman, *J. Am. Chem. Soc.* 103 (1981) 4126;  
(c) W.A. Gustavson, L.M. Principe, W.-Z. Min Rhee, J.J. Zuckerman, *Inorg. Chem.* 20 (1981) 3460.
- [65] M. Saito, R. Haga, M. Yoshioka, *Heteroatom. Chem.* 12 (2001) 349.
- [66] M. Saito, R. Haga, M. Yoshioka, *Chem. Commun.* (2002) 1002.
- [67] H. Sohn, *J. Organomet. Chem.* 689 (2004) 134.
- [68] T. Gans-Eichler, D. Gudat, M. Nieger, *Angew. Chem. Int. Ed.* 41 (2002) 1888.
- [69] M. Saito, R. Haga, M. Yoshioka, *Chem. Lett.* 32 (2003) 912.
- [70] M. Wakasa, T. Kugita, *Organometallics* 17 (1998) 1913.
- [71] N. Wiberg, H. Schuster, A. Simon, K. Peters, *Angew. Chem. Int. Ed.* 25 (1986) 79.